

Research

Open Access

Systematisation of spatial uncertainties for comparison between a MR and a CT-based radiotherapy workflow for prostate treatments

Tufve Nyholm*¹, Morgan Nyberg², Magnus G Karlsson³ and Mikael Karlsson⁴

Address: ¹Department of radiation sciences (Oncology), Umeå University Hospital, 90187 Umeå, Sweden, ²Information and Communication Technology, Luleå University of Technology, Sweden, ³Department of radiation physics, Umeå University Hospital, 90185 Umeå, Sweden and ⁴Radiation physics section, Department of radiation sciences, Umeå University, 90187 Umeå, Sweden

Email: Tufve Nyholm* - tufve.nyholm@radfys.umu.se; Morgan Nyberg - morgan.nyberg@itu.se; Magnus G Karlsson - magnus.g.karlsson@vll.se; Mikael Karlsson - mikael.karlsson@radfys.umu.se

* Corresponding author

Published: 17 November 2009

Received: 28 August 2009

Radiation Oncology 2009, **4**:54 doi:10.1186/1748-717X-4-54

Accepted: 17 November 2009

This article is available from: <http://www.ro-journal.com/content/4/1/54>

© 2009 Nyholm et al; licensee BioMed Central Ltd.

This is an Open Access article distributed under the terms of the Creative Commons Attribution License (<http://creativecommons.org/licenses/by/2.0>), which permits unrestricted use, distribution, and reproduction in any medium, provided the original work is properly cited.

Abstract

Background: In the present work we compared the spatial uncertainties associated with a MR-based workflow for external radiotherapy of prostate cancer to a standard CT-based workflow. The MR-based workflow relies on target definition and patient positioning based on MR imaging. A solution for patient transport between the MR scanner and the treatment units has been developed. For the CT-based workflow, the target is defined on a MR series but then transferred to a CT study through image registration before treatment planning, and a patient positioning using portal imaging and fiducial markers.

Methods: An "open bore" 1.5T MRI scanner, Siemens Espree, has been installed in the radiotherapy department in near proximity to a treatment unit to enable patient transport between the two installations, and hence use the MRI for patient positioning. The spatial uncertainty caused by the transport was added to the uncertainty originating from the target definition process, estimated through a review of the scientific literature. The uncertainty in the CT-based workflow was estimated through a literature review.

Results: The systematic uncertainties, affecting all treatment fractions, are reduced from 3-4 mm (1Sd) with a CT based workflow to 2-3 mm with a MR based workflow. The main contributing factor to this improvement is the exclusion of registration between MR and CT in the planning phase of the treatment.

Conclusion: Treatment planning directly on MR images reduce the spatial uncertainty for prostate treatments.

Background

MR images are well suited for target delineation, not only for the prostate [1], but also for many other tumours, such as brain lesions [2,3] and head and neck tumours [4,5], which explains the growing interest for MR in radiother-

apy [6-12]. An "open bore" 1.5T MRI, has been installed in direct connection to a treatment unit at the radiotherapy department in Umeå [13]. This installation allows us to image most of our patients in treatment position with the MR for the target delineation, and open the door for

development of an online treatment setup workflow designed for soft tissue tumours. Figure 1 illustrates a MR-only workflow and a more conventional CT-based workflow. In the MR-based workflow, the target definition, the treatment planning, and patient positioning at treatment delivery, are performed with MR aid only. The patient positioning utilize a transport trolley to move the patient from the imaging in the MR to the treatment table. A very robust fixation of the patient provides control over the relation among the coordinate systems in the patient, in the MR, and in the treatment room. However, the transport does introduce uncertainties, which must be accounted for in an evaluation of the workflow and the resulting geometric uncertainties.

An alternative workflow could be to plan on MR material followed by positioning based on fiducial markers. This intermediate workflow requires that the internal markers are visible on the MR images and that the apparent marker positions are correct. Parker et al. [14] shows that internal markers appear clearly on gradient echo sequences, while more difficulty to identify on T2-weighted turbo spin echo sequences. The visibility of the markers was increased when the TE time was reduced, giving higher signal but compromising the T2-weighted contrast. Verified robust imaging of fiducial markers in MR would enable also this workflow. In the present study, this intermediate workflow will not be explicitly handled.

The purpose of this study is to investigate if a MR-only radiotherapy workflow, in accordance with figure 1b, has the potential to improve the spatial accuracy compared to the more conventional CT-based workflow (figure 1a). The estimations of the uncertainties in the different work-

flows are based on both a literature review and the results of our own experiments.

Methods

In order to assess the total spatial uncertainties in the two workflows, shown in figure 1, the workflow processes were broken down into independent sub processes. Both workflows contain two main steps where uncertainties can be introduced, target definition for treatment planning and patient positioning at treatment delivery. Our tools in the uncertainty analysis have been literature reviews, and when necessary own experiments. The own experiments concern positioning with MRI, and are described in the section about MR guided delivery.

An open-bore MRI scanner (Siemens Espree, 1.5T) was used for the MR imaging of the patients in connection radiotherapy. For prostate patients, a T2-weighted SPACE sequence (Siemens), which is a 3D turbo spin-echo sequence with varying flip angle on the refocusing pulses, was used. The slice thickness was 1.7 mm, typical pixel-size was $1.0 \times 1.0 \text{ mm}^2$, and the bandwidth was 592 Hz per pixel. Distortions caused by gradient non-linearity were corrected with an algorithm based on spherical harmonic expansion of the fields generated by the gradient coils [15]. The 3D correction algorithm including representation of the coils was delivered by Siemens as a standard clinical tool integrated in the scanner software (VB15). The scanner was set in an isocentric mode, which moves the table prior to the acquisition of each sequence, to place the MR isocenter in the centre of the volume of interest.

The total spatial uncertainty consists of both a random part, varying in direction and magnitude from fraction to fraction, and a systematic part, which is invariant over the treatment period. The systematic and random uncertainty should be given different weight in the formation of margins between the CTV and the PTV. In the present work we used the weight factor 2.5 for the systematic errors and 0.7 for random errors as proposed by van Herk et. al. [16,17]. The PTV margin is hence expressed as

$$m_{\text{PTV}} = 2.5 \Sigma + 0.7\sigma \quad (1)$$

where Σ is the systematic and σ is the random spatial uncertainty. The presented uncertainties are throughout this paper presented in units of one standard deviation (1SD), thus inherently assuming normal distributed data.

Uncertainty in target definition

The total uncertainty in the target definition can be broken down to three subparts: uncertainty in prostate delineation (MR-based on both workflows), spatial distortion in MR images that can be scanner related and patient

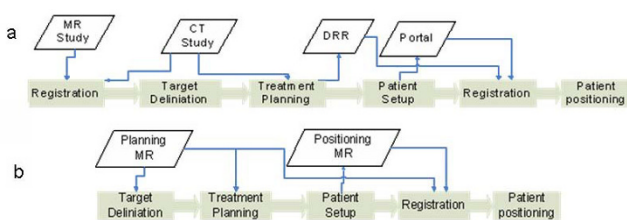


Figure 1
Overview of the two workflows analyzed in the present study. (a) A widely used workflow utilizing registration between MR and CT images in order to transfer the delineated prostate volume (GTV/CTV) from the MR study to the CT study. The CT study is used for treatment planning and to generate DRR's for patient position. Typically, fiducial markers are used. (b) The workflow is entirely based on MR, both for planning and positioning.

induced, and for the CT-based workflow: uncertainty in registration between CT and MR images.

Uncertainty in prostate delineation

Rasch et al [18] has from a study with 18 patient analysed by 3 physicians reported an uncertainty, in the prostate delineation on axial MR study, of 2 mm at the base of seminal vesicles and up to 2.8 mm in the prostate apex. The uncertainty in the head-foot (HF) direction was 2.5 mm with a slice thickness of 5-6 mm for the axial MR images. In a later study involving 7 physicians analysing 10 patients Smith et al. [19] reported a radial uncertainty of 0.6 - 1.6 mm for the delineation of the prostate where the larger value is for the apex. The inter-observer uncertainty in the length (HF direction) of the prostate was 3.4 mm, and the intra-observer variation was 2.6 mm; the slice thickness was 2.5 mm.

In summary, the literature review indicates a prostate delineation uncertainty of 1.8 mm in the right-left (RL) and anterior-posterior (AP) directions and 2.8 mm in the HF direction.

Geometrical Distortions in MR

Geometrical distortions in MR images are a well known phenomena [20-22]. In modern MR scanners, gradient non-linearity is the main cause of image distortions [20], dominating over the effect of static field inhomogeneity. The distortions introduced by the gradient non-linearities are increasing with the distance from the MR isocenter [20,23]. Without correction, the geometrical distortions in modern MR scanners can cause deviations between physical and imaged distances of up to 20% in extreme situations. However, there are methods for distortion correction which reduces the errors significantly. It is possible to use a specially designed geometry phantom to characterize and correct the distortions for a specific scanner [22,24]. In the present work, a gradient coil specific distortion correction algorithm was applied. Even though this device specific corrections only correct for intrinsic gradient non-linearity connected to a specific type of scanner/gradient coil, it has been shown that this kind of correction yields a spatial accuracy better than 2% [23,25], which is sufficient when region of interest in the patient is close to the MR isocenter. Patient anatomy, e.g. air pockets in the rectal cavity, can generate susceptibility-generated field changes up to ± 10 ppm [26]. With a bandwidth of 592 Hz per pixel this corresponds to distortions up to approximately 1 pixel for a 1.5T scanner. Thus, magnetic susceptibility related distortions are a minor effect for the sequence used.

In summary, for a prostate with radius of 2.5 cm the geometrical distortions can cause errors of up to 0.5 mm, which corresponds to a standard deviation of around 0.2

mm. This uncertainty is approximately equal in all directions provided that a 3D correction algorithm is used.

Registration uncertainties - MR/CT

The workflow in figure 1a involves a registration between a CT and MR study. Errors in this registration directly affect the spatial accuracy of the target definition. Registrations between MR and CT for prostate patients can be performed based on fiducial markers [14]. The trend is, however, to use mutual information (MI) registration based directly on the patient anatomy [27,28]. The prostate position relative other anatomical structures is not fixed, therefore the registration should ideally be based on the prostate with just a small margin. However, this has been reported problematic because of too limited morphological information content in the CT representation of the prostate [29,30]. A few studies have been performed evaluating the accuracy and precision of MI registration for CT and MR studies of the prostate; the registration uncertainty has been reported to be around 2 mm [29,31]. Roberson et al. [31] reported that registration results depend on the starting point for a specific MI optimization software. The mean difference between different starting points was up to 1 mm in the RL direction. The corresponding number for MR-MR registration was 0.4 mm in the HF direction which could indicate that the mutual information maximum is more distinct for MR-MR registration compared to CT-MR registration.

In summary, the registration uncertainty for a CT - MR registration for a prostate case was estimated to be 2 mm based on current reports in the scientific literature.

Uncertainty in patient positioning

The patient positioning at treatment, with the development of image guided radiotherapy, been in focus the recent years. For prostate cancer patients the improvements in spatial treatment accuracy has been considerable. Both the CT and the MR-based workflows, shown in figure 1, rely on imaging before each fraction. Intra-fraction motion of the prostate is therefore an issue for both workflows.

Intra-fraction prostate motion

In a large investigation by Kotte et al [32] intra fraction motion larger than 2 mm was observed during 66% of the fractions, this number is roughly in agreement with the results presented in other studies [33,34]. However, reduction of the rectal filling has been showed to be of great importance to achieve a stable prostate position [33,35]; an uncertainty of 2 mm is therefore realistic for a 5-7 min treatment when patients are instructed to empty rectum prior to treatment. The position uncertainty due to prostate motion is most pronounced in the AP and HF directions [32,36].

In summary, the overall uncertainty for the prostate position was estimated to 2 mm, which broken down in the orthogonal directions corresponds to: 1.4 mm in AP and HF, and 0.4 mm in RL.

Uncertainty with fiducial markers

There are numerous studies on the accuracy of patient positioning using fiducial markers and portal or flat screen kV images. Several different sources of uncertainty need to be considered in order to correctly estimate the overall accuracy of the workflow. Random positioning errors are partly due to uncertainty in the registration between the reference image and the portal/kV flat screen image. Literature indicates that a manual registration typically results in uncertainty of around 0.7 mm in the HF and RL direction, and 1.4 mm in the AP direction [37,38].

An investigation by Nichol et al [39] indicates that a systematic deformation of the prostate during radiotherapy leads to drift in the relation between the centre of mass for the markers and centre of mass for the contoured prostate. This uncertainty is in the order of 1 mm, which is roughly in agreement with other reports [40,41]. It should be noted that deformation of the prostate is in many respects equivalent to marker migration within the prostate. These two effects are therefore not separated in the present work. Prostate deformation and marker migration are resulting in a systematic uncertainty in the patient position.

The uncertainty of clinical imaging systems are in the order of 1 mm, accounting for limitations in resolution, isocenter position and mechanical instability. Paulsen et al [34] observed a systematic discrepancy of almost 1 mm when comparing 2 different imaging modalities at 2 different accelerators. Kotte et al. [32] detected that the sag of the gantry caused a systematic imaging deviations of almost 1 mm in the HF direction when the gantry was in 0 degree position compared to 180 degree position.

In summary, it is estimated that the uncertainty in the day to day registrations between reference image and the portal image is 0.7 mm in RL and HF direction and 1.4 mm in AP direction. The estimated uncertainty for the marker position in the prostate is 1 mm in all directions, and the estimated total uncertainty for the imaging systems is 1 mm in all directions.

MR guided treatment delivery

The MR positioning approach is novel; we therefore describe the principals in detail below, as well as the experiments performed to estimate the uncertainties connected to the method.

Figure 2 shows the hardware configuration. The patient is transported between the MR scanner and the treatment unit on a MR compatible trolley (Miyabi, TRUMPF). The

patient is fixated on a shell, with a double vacuum system (BodyFIX, Medical Intelligence an Elekta company), which can be slid from the trolley to the treatment or MR table after docking. The shell has fixed positions both at the MR and the treatment table, which enables absolute coordinate transformation between MR coordinates and treatment coordinates. The treatment table is a Siemens 550 TxT equipped with a modified TT-D table-top compatible with the Miyabi transport solution. The daily treatment table coordinates are calculated as the absolute table coordinates from the treatment planning corrected for daily variations in patient and prostate position. The daily correction is calculated based on a sub-volume-based rigid mutual information registration between the reference MR images used at treatment planning and daily positioning MR images. The same SPACE sequence was used both for treatment planning and for daily positioning. Calibration of the system, i.e. determination of the absolute coordinate transformation vector, is an obvious source for systematic uncertainty, while mechanical instabilities in the mounting mechanism at the MR and treatment table together with image distortion, image registration errors and patient movement during transport mainly result in uncertainty of random nature.

Uncertainty in calibration vector determination

The calibration vector is the relation between the coordinate for a specific point, in the MR coordinate system and the treatment table coordinates that brings the same point to the treatment isocenter. The calibration vector was determined using a phantom which is sketched in figure 3. The centre point of the phantom is clearly visible on MR, CT, portal images and can also be positioned using lasers. We placed the phantom at various positions on the Miyabi shell and carefully determined the position of the centre point in both the MR coordinate system using MR images, and the treatment coordinate system using calibrated lasers. The calibration vector was calculated, for each phantom position on the Miyabi shell, as the difference between the MR coordinates and the treatment table coordinates for the central point in the phantom. The idea with repeated measurements was to assess the precision of the vector determination taking intrinsic inhomogeneities in the magnetic field and position dependent distortions into account. In total 16 independent determinations of the calibration vector was performed, for different phantom positions on the Miyabi shell. The measurements were performed with the phantom centre positioned at ± 25 mm in the AP direction, and ± 60 mm in the RL direction and at 4 different positions along the HF direction with a total span of 450 mm. The scanning of the phantom was performed in isocentric mode.

Weight correction

The calibration vector needs to be corrected based on the patient's weight to account for the treatment table sag-

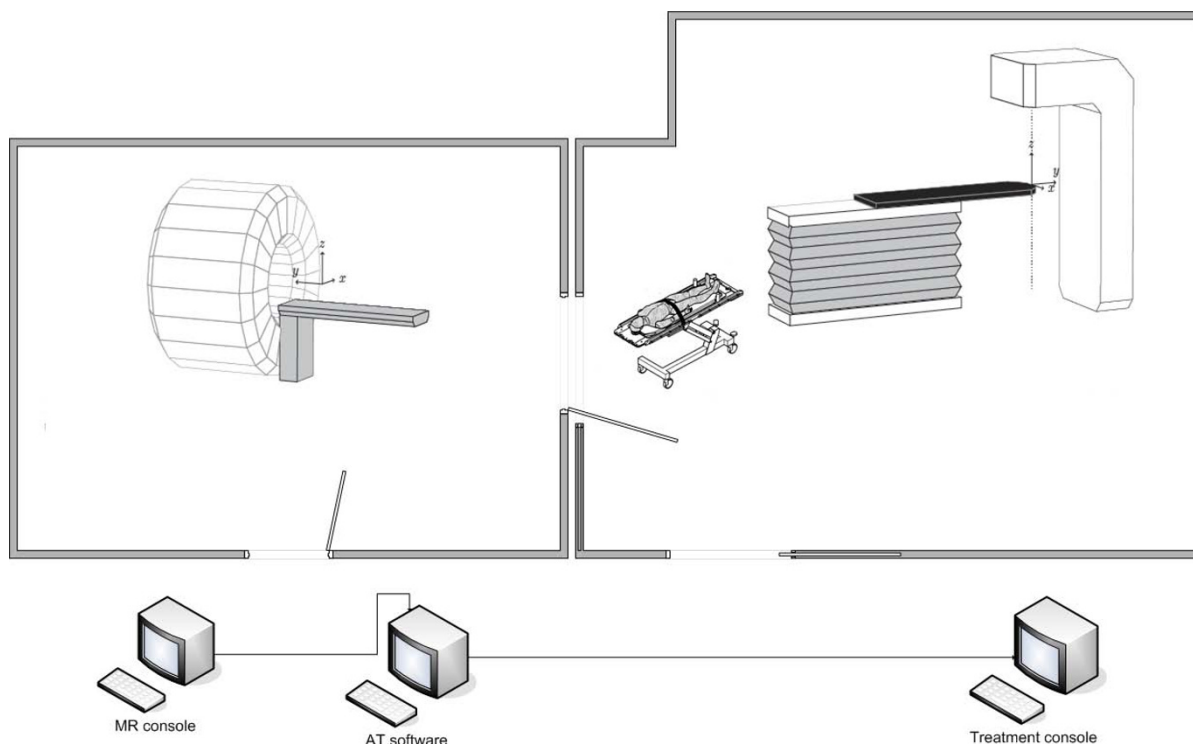


Figure 2

Schematic overview of the hardware configuration for the MR positioning of patients. There is a direct connection between the MR room and treatment room, which makes patient transport quick and simple. In parallel with the patient transport the treatment couch coordinates are calculated using dedicated image registration software, the transport in it self does therefore not prolong the procedure.

ging. The magnitude of the sagging was investigated using a set of 15 kg bricks which were distributed to approximate the weight distribution of a typical patient. We varied the total load and the weight distribution on the table top, to simulate patient weight from 0 to 105 kg, and patient height from approximately 150 cm to 190 cm.

Geometrical distortions

The prostate is typically located on the patient's central line and with the Miyabi shell together with the BodyFIX vacuum pillow the height of the prostate for the typical patient will be very close to the isocenter. The internal MR laser is used to position the patient in the HF direction before imaging, thus the prostate will be close to the isocenter also in the HF direction. If the prostate centre is within a sphere of 5 cm around the MR isocenter and the maximum spatial distortion is 2% then the maximum error will be approximately 1 mm, i.e. a standard deviation around 0.5 mm. The geometrical distortions systematically affect the entire treatment through the reference images, and do in addition contribute to random errors at each fraction.

Patient movement

Significant patient movements during the time interval from the imaging to the treatment are deemed highly unlikely when using the double vacuum immobilization device. There is however a risk for prostate movements within the body during this time interval as discussed above (see section about intra-fraction prostate movement)

Position reproducibility

The reproducibility of the Miyabi shell position on the MR and treatment table were investigated through measurement of the maximum shell displacement under direct force in different directions

Registration uncertainties MR/MR

The registration accuracy with mutual information algorithms has been discussed above in the section about uncertainty in target definition. Based on the high soft tissue contrast in the MR images and the similar information content in the reference and positioning image it was assumed that the accuracy is limited by the size of the voxels. A voxel size of $1.0 \times 1.0 \times 2.5 \text{ mm}^3$ gives a registration

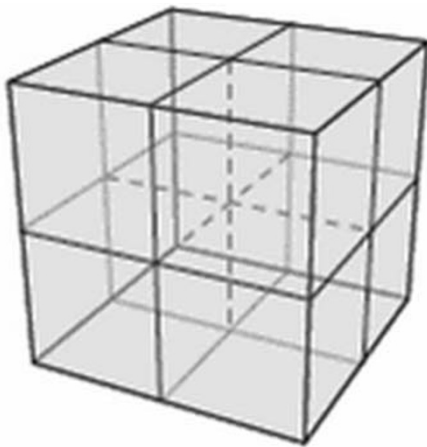


Figure 3 Calibration phantom. The phantom which was used for coordinate calibration is 15 × 15 × 15 cm³ and filled with water. The central point is defined with lead bullet of 1 mm diameter which is fasten with 6 thin plexi rods creating a 3D hair cross.

uncertainty of 0.5, 0.5, and 1.25 mm in the RL, AP and HF directions respectively.

Results

Uncertainties associated with MR transport

Calibration vector

The calibration vector relates the coordinate system in the MR scanner with the treatment table coordinate system. The estimated uncertainty for the calibration vector, based on the 16 independent measurements, was 0.5 mm, 0.4 mm resp. 0.8 mm in the RL, HF and AP directions. The mean value of the 16 observations is connected to a systematic uncertainty of 0.1 to 0.2 mm.

Correction for weight

The calibration vector was measured without load. Therefore there is a need to correct for the sagging of the treatment table under the weight of the patient. We found that the sagging of the treatment table could be modelled as a linear function of the patient weight (*w*) and the longitudinal coordinate for the prostate (*l*) in the MR coordinate system, according to:

$$\delta_z = -0.000178 * w * (l - 1178.6) \quad (2)$$

where the units are kg and mm respectively.

For simulated patients in the weight interval between 60 and 110 kg with their prostate located approximately 700-900 mm from the top of the skull, residual errors of maximum 1.2 mm was observed in the AP direction (figure 4), and 0.4 mm in the HF direction. In general the residual errors were small and the standard deviation of this sys-

tematic uncertainty was estimated to 0.6 mm in the AP direction, 0.2 mm in the HF direction, and neglectable in the RL direction.

Position reproducibility

Under direct force it was possible to displace the Miyabi shell slightly below 1 mm in the HF direction; this maximum displacement corresponds to an uncertainty under normal distribution assumption of around 0.5 mm. It was not possible to measure any positioning inaccuracies in the RL and AP directions. The uncertainty in the HF direction results in systematic uncertainties in the imaging for the treatment planning with a magnitude of 0.5 mm, and does in addition result in fraction to fraction positioning uncertainties of 0.7 mm (both MR and treatment table docking).

Comparison with established technique

Table 1 summarizes results from the literature review in section 3 and results presented in section 4. The total estimated positioning uncertainty for a CT-based workflow, illustrated in figure 1a, is substantially larger than the estimated uncertainty using the MR-based workflow (figure 1b). The clinical implication of spatial uncertainties is the use of margins, dependent on both the random and systematic part. In the present work we use the model described through equation (1). The CT-based workflow should according to equation (1) be associated with the following margins: RL - 8.1 mm, AP - 8.7 mm, and HF - 10.7 mm. The corresponding margin for the MR-based workflow should be: RL - 5.3 mm, AP - 6.1 mm, and HF - 8.7 mm.

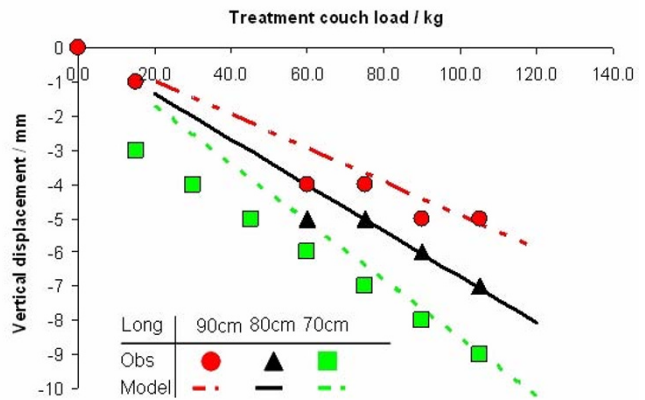


Figure 4 Sagging of treatment table. Modelled table sagging, the lines, is compared with observed sag, the points, for different simulated patient weights and prostate positions. The parameter "Long" describes the distance from the head end of the Miyabi shell to the prostate.

Table 1: Estimated positioning uncertainties CT resp. MR based treatment procedure

| Contributing factor | CT based workflow | | | | | | MR based workflow | | | | | |
|---|-------------------|----------------|----------------|----------------|----------------|-----------------|-------------------|----------------|----------------|----------------|----------------|----------------|
| | CT/MR-systematic | | | CT/MR-Random | | | MR-systematic | | | MR-random | | |
| | Σ RL mm | Σ AP mm | Σ HF mm | σ RL Mm | σ AP mm | σ gHF mm | Σ RL mm | Σ AP mm | Σ HF mm | σ RL mm | σ AP mm | σ HF mm |
| Prostate delineation | 1.8 | 1.8 | 2.8 | ---- | ---- | ---- | 1.8 | 1.8 | 2.8 | ---- | ---- | ---- |
| Geometrical distortions | 0.2 | 0.2 | 0.2 | ---- | ---- | ---- | 0.2 | 0.2 | 0.2 | ---- | ---- | ---- |
| MR to CT registration | 2 | 2 | 2 | ---- | ---- | ---- | ---- | ---- | ---- | ---- | ---- | ---- |
| Total treatment planning uncertainty | 2.7 | 2.7 | 3.4 | ---- | ---- | ---- | 1.8 | 1.8 | 2.8 | ---- | ---- | ---- |
| Intra-fraction motion | ---- | ---- | ---- | 0.4 | 1.4 | 1.4 | ---- | ---- | ---- | 0.4 | 1.4 | 1.4 |
| CT to X-ray registration | ---- | ---- | ---- | 0.7 | 0.7 | 1.4 | ---- | ---- | ---- | ---- | ---- | ---- |
| Fidutial marker uncertainty | 1.0 | 1.0 | 1.0 | ---- | ---- | ---- | ---- | ---- | ---- | ---- | ---- | ---- |
| X-ray Imaging uncertainty | 1.0 | 1.0 | 1.0 | ---- | ---- | ---- | ---- | ---- | ---- | ---- | ---- | ---- |
| MR Imaging uncertainty/distortion | ---- | ---- | ---- | ---- | ---- | ---- | 0.5 | 0.5 | 0.5 | 0.5 | 0.5 | 0.5 |
| MR to MR registration | ---- | ---- | ---- | ---- | ---- | ---- | ---- | ---- | ---- | 0.5 | 0.5 | 1.25 |
| Calibration vector determination | ---- | ---- | ---- | ---- | ---- | ---- | 0.1 | 0.2 | 0.1 | ---- | ---- | ---- |
| Weight correction | ---- | ---- | ---- | ---- | ---- | ---- | ---- | 0.6 | 0.2 | ---- | ---- | ---- |
| Docking mechanism | ---- | ---- | ---- | ---- | ---- | ---- | ---- | ---- | 0.5 | ---- | ---- | 0.7 |
| Total Set-up uncertainty | 1.4 | 1.4 | 1.4 | 0.8 | 1.6 | 2.0 | 0.5 | 0.8 | 0.7 | 0.8 | 1.6 | 2.1 |
| Total uncertainty | 3.0 | 3.0 | 3.7 | 0.8 | 1.6 | 2.0 | 1.9 | 2.0 | 2.9 | 0.8 | 1.6 | 2.1 |

Discussion

Through this literature review together with our analysis of the positioning procedure with MR, we claim that the MR-only treatment workflow, shown in figure 1b, allows for significantly smaller PTV margins than the CT-based workflow (figure 1a). This conclusion has been reached through estimations of the uncertainty for each sub process in the treatment chain and sum-up's of the total spatial uncertainty assuming that the errors from the sub processes are uncorrelated. This method yields results comparable to other studies, for example, the resulting margins for the positioning using CT-based workflow and gold markers are comparable with the results presented by Beltran et al. [42]. Excluding the uncertainty in the delineation of the prostate both Beltran et al. and the present study estimate the proper margins to between 4 mm and 5 mm in all directions. The contributions from different sources of uncertainty do however differ.

The reduced uncertainty does not necessarily mean that MR-only is the optimal workflow as other aspects also needs to be considered. It is not feasible to introduce a positioning method which requires considerably more patient time for all the 30-40 fractions than what are standard at many departments. However, the importance of occupation time per treatment would be reduced if the hypo-fractionation of prostate treatments becomes clinical standard.

The delineation uncertainty is dominating the systematic overall uncertainty also for the MR only workflow. It is clear that more effort needs to be spent on reducing uncertainty in the target delineation procedure.

In the present study we have used a generic algorithm for 3D distortions correction provided as a standard routine in the VB15 package delivered by Siemens. The accuracy of this correction was validated using a Philips PIQT phantom, through comparison with CT and through direct distance measurements in the images. The results were in agreement with the results reported by Krager et al. [23]. It can be expected that the accuracy of generic distortion correction algorithms may vary between individual scanners, it is thus important to validate the geometrical accuracy for each MR-scanner before any clinical implementation. Equally important is verification of the site specific registration accuracy, which can differ depending of algorithm, region of interest, and clinical implementation. The uncertainty quantification presented in Table 1 are representative for the described methodology, but should be verified locally.

Registrations between MR and CT, and MR to MR, were in the present study performed using a MI based method. An alternative workflow uses the internal gold markers as reference points in a landmark based registration. This regis-

tration method was not included in the present study for several reasons. -The markers are not clearly visible with the T2 weighted 3D sequence that is we use for target delineation. -Introduction of a dedicated sequence for visualization of the markers gives a systematic spatial uncertainty because of prostate movement between the sequences. -Use of a multi-echo sequence to acquire both T2 weighted images for delineation and proton density weighted images for visualization of the markers compromise the quality of the images used for delineation compared to present 3D sequence. -Finally, there is still a need for an in-depth investigation of the spatial uncertainties in the apparent marker position in the MR images, specifically, with respect to variations in frequency encoding direction, bandwidth, slice encoding method, and marker shape and orientation relative the main magnetic field.

Conclusion

It was shown that, from a spatial uncertainty point of view, the MR-only prostate treatment workflow is to be preferred in front of a MR/CT-based procedure. The systematic uncertainties introduced by the MR/CT-registration are affecting the entire treatment but are avoided with the MR-based workflow, while the random uncertainties from fraction to fraction are approximately the same as for the MR/CT workflow.

Competing interests

The authors declare that they have no competing interests.

Authors' contributions

TN Participated in the design of the study participated in the literature review and drafted the manuscript. MN Participated in the design of the study and performed the experimental work

MGK Participated in the design of the study and in the literature review. MK Participated in the design of the study and in the literature review. All authors read and approved the final manuscript

Acknowledgements

We thank Cenneth Forsmark for the construction of the equipment, Magnus Karlsson (Siemens Healthcare, Sweden) for discussions and comments, and the Swedish Cancer Society and the Cancer Research Foundation North Sweden for financial support.

References

1. Hricak H: **MR imaging and MR spectroscopic imaging in the pre-treatment evaluation of prostate cancer.** *Br J Radiol* 2005, **78(Spec No 2)**:S103-111.
2. Hawighorst H, Debus J, Schreiber W, Knopp MV, Engenhart-Cabillic R, Essig M, Brix G, van Kaick G: **Contrast-enhanced magnetization transfer imaging: improvement of brain tumor conspicuity and delineation for radiosurgical target volume definition.** *Radiother Oncol* 1997, **43(3)**:261-7.
3. Prabhakar R, Haresh KP, Ganesh T, Joshi RC, Julka PK, Rath GK: **Comparison of computed tomography and magnetic resonance based target volume in brain tumors.** *J Cancer Res Ther* 2007, **3(2)**:121-3.

4. Rasch C, Steenbakkers R, van Herk M: **Target definition in prostate, head, and neck.** *Semin Radiat Oncol* 2005, **15(3)**:136-45.
5. Krempien RC, Daeuber S, Hensley FW, Wannenmacher M, Harms W: **Image fusion of CT and MRI data enables improved target volume definition in 3D-brachytherapy treatment planning.** *Brachytherapy* 2003, **2(3)**:164-71.
6. Pasquier D, Betrouni N, Vermandel M, Lacornerie T, Lartigau E, Rousseau J: **MRI alone simulation for conformal radiation therapy of prostate cancer: technical aspects.** *Conf Proc IEEE Eng Med Biol Soc* 2006, **1**:160-3.
7. Chen L, Nguyen TB, Jones E, Chen Z, Luo W, Wang L, Price RA Jr, Pollack A, Ma CM: **Magnetic resonance-based treatment planning for prostate intensity-modulated radiotherapy: creation of digitally reconstructed radiographs.** *Int J Radiat Oncol Biol Phys* 2007, **68(3)**:903-11.
8. Chen L, Price RA Jr, Nguyen TB, Wang L, Li JS, Qin L, Ding M, Palacio E, Ma CM, Pollack A: **Dosimetric evaluation of MRI-based treatment planning for prostate cancer.** *Phys Med Biol* 2004, **49(22)**:5157-70.
9. Chen L, Price RA Jr, Wang L, Li J, Qin L, McNeeley S, Ma CM, Freedman GM, Pollack A: **MRI-based treatment planning for radiotherapy: dosimetric verification for prostate IMRT.** *Int J Radiat Oncol Biol Phys* 2004, **60(2)**:636-47.
10. Chen Z, Ma CM, Paskalev K, Li J, Yang J, Richardson T, Palacio L, Xu X, Chen L: **Investigation of MR image distortion for radiotherapy treatment planning of prostate cancer.** *Phys Med Biol* 2006, **51(6)**:1393-403.
11. Raaijmakers AJ, Raaijmakers BW, Meer S van der, Lagendijk JJ: **Integrating a MRI scanner with a 6 MV radiotherapy accelerator: impact of the surface orientation on the entrance and exit dose due to the transverse magnetic field.** *Phys Med Biol* 2007, **52(4)**:929-39.
12. Lagendijk JJ, Raaijmakers BW, Raaijmakers AJ, Overweg J, Brown KJ, Kerkhof EM, Put RW van der, Hardemark B, van Vulpen M, Heide UA van der: **MR/linac integration.** *Radiother Oncol* 2008, **86(1)**:25-9.
13. Karlsson M, Karlsson MG, Nyholm T, Amies C, Zackrisson B: **Dedicated MR in the Radiotherapy clinic.** *Int J Radiat Oncol Biol Phys* 2009, **74(2)**:644-51.
14. Parker CC, Damyonovich A, Haycocks T, Haider M, Bayley A, Catton CN: **Magnetic resonance imaging in the radiation treatment planning of localized prostate cancer using intra-prostatic fiducial markers for computed tomography co-registration.** *Radiother Oncol* 2003, **66(2)**:217-24.
15. Janke A, Zhao H, Cowin GJ, Galloway GJ, Doddrell DM: **Use of spherical harmonic deconvolution methods to compensate for nonlinear gradient effects on MRI images.** *Magn Reson Med* 2004, **52(1)**:115-22.
16. van Herk M, Remeijer P, Rasch C, Lebesque JV: **The probability of correct target dosage: dose-population histograms for deriving treatment margins in radiotherapy.** *Int J Radiat Oncol Biol Phys* 2000, **47(4)**:1121-35.
17. van Herk M: **Errors and margins in radiotherapy.** *Semin Radiat Oncol* 2004, **14(1)**:52-64.
18. Rasch C, Barillot I, Remeijer P, Touw A, van Herk M, Lebesque JV: **Definition of the prostate in CT and MRI: a multi-observer study.** *Int J Radiat Oncol Biol Phys* 1999, **43(1)**:57-66.
19. Smith WL, Lewis C, Bauman G, Rodrigues G, D'Souza D, Ash R, Ho D, Venkatesan V, Downey D, Fenster A: **Prostate volume contouring: a 3D analysis of segmentation using 3DTRUS, CT, and MR.** *Int J Radiat Oncol Biol Phys* 2007, **67(4)**:1238-47.
20. Wang D, Strugnell W, Cowin G, Doddrell DM, Slaughter R: **Geometric distortion in clinical MRI systems Part I: evaluation using a 3D phantom.** *Magn Reson Imaging* 2004, **22(9)**:1211-21.
21. Wang D, Strugnell W, Cowin G, Doddrell DM, Slaughter R: **Geometric distortion in clinical MRI systems Part II: correction using a 3D phantom.** *Magn Reson Imaging* 2004, **22(9)**:1223-32.
22. Wang D, Doddrell DM, Cowin G: **A novel phantom and method for comprehensive 3-dimensional measurement and correction of geometric distortion in magnetic resonance imaging.** *Magn Reson Imaging* 2004, **22(4)**:529-42.
23. Karger CP, Hoss A, Bendl R, Canda V, Schad L: **Accuracy of device-specific 2D and 3D image distortion correction algorithms for magnetic resonance imaging of the head provided by a manufacturer.** *Phys Med Biol* 2006, **51(12)**:N253-61.
24. Doran SJ, Charles-Edwards L, Reinsberg SA, Leach MO: **A complete distortion correction for MR images: I. Gradient warp correction.** *Phys Med Biol* 2005, **50(7)**:1343-61.
25. Jovicich J, Czanner S, Greve D, Haley E, Kowke A van der, Gollub R, Kennedy D, Schmitt F, Brown G, Macfall J, Fischl B, Dale A: **Reliability in multi-site structural MRI studies: effects of gradient non-linearity correction on phantom and human data.** *Neuroimage* 2006, **30(2)**:436-43.
26. Schenck JF: **The role of magnetic susceptibility in magnetic resonance imaging: MRI magnetic compatibility of the first and second kinds.** *Med Phys* 1996, **23(6)**:815-50.
27. Maes F, Collignon A, Vandermeulen D, Marchal G, Suetens P: **Multi-modality image registration by maximization of mutual information.** *IEEE Trans Med Imaging* 1997, **16(2)**:187-98.
28. Wells WM, Viola P, Atsumi H, Nakajima S, Kikinis R: **Multi-modal volume registration by maximization of mutual information.** *Med Image Anal* 1996, **1(1)**:35-51.
29. McLaughlin PW, Narayana V, Kessler M, McShan D, Troyer S, Marsh L, Hixson G, Roberson PL: **The use of mutual information in registration of CT and MRI datasets post permanent implant.** *Brachytherapy* 2004, **3(2)**:61-70.
30. Vidakovic S, Jans HS, Alexander A, Sloboda RS: **Post-implant computed tomography-magnetic resonance prostate image registration using feature line parallelization and normalized mutual information.** *J Appl Clin Med Phys* 2007, **8(1)**:21-32.
31. Roberson PL, McLaughlin PW, Narayana V, Troyer S, Hixson GV, Kessler ML: **Use and uncertainties of mutual information for computed tomography/magnetic resonance (CT/MR) registration post permanent implant of the prostate.** *Med Phys* 2005, **32(2)**:473-82.
32. Kotte AN, Hofman P, Lagendijk JJ, van Vulpen M, Heide UA van der: **Intrafraction motion of the prostate during external-beam radiation therapy: analysis of 427 patients with implanted fiducial markers.** *Int J Radiat Oncol Biol Phys* 2007, **69(2)**:419-25.
33. Ghilezan MJ, Jaffray DA, Siewerdsen JH, Van Herk M, Shetty A, Sharpe MB, Zafar Jafri S, Vicini FA, Matter RC, Brabbin DS, Martinez AA: **Prostate gland motion assessed with cine-magnetic resonance imaging (cine-MRI).** *Int J Radiat Oncol Biol Phys* 2005, **62(2)**:406-17.
34. Poulsen PR, Muren LP, Hoyer M: **Residual set-up errors and margins in on-line image-guided prostate localization in radiotherapy.** *Radiother Oncol* 2007, **85(2)**:201-6.
35. Fiorino C, Di Muzio N, Broggi S, Cozzarini C, Maggiulli E, Alongi F, Valdagni R, Fazio F, Calandrino R: **Evidence of Limited Motion of the Prostate by Carefully Emptying the Rectum as Assessed by Daily MVCT Image Guidance with Helical Tomotherapy.** *Int J Radiat Oncol Biol Phys* 2008, **1;71(2)**:611-7.
36. Britton KR, Takai Y, Mitsuya M, Nemoto K, Ogawa Y, Yamada S: **Evaluation of inter- and intrafraction organ motion during intensity modulated radiation therapy (IMRT) for localized prostate cancer measured by a newly developed on-board image-guided system.** *Radiat Med* 2005, **23(1)**:14-24.
37. Berthelet E, Truong PT, Zavgorodni S, Moravan V, Liu MC, Runkel J, Bendorff B, Sayers D: **Consistency in electronic portal imaging registration in prostate cancer radiation treatment verification.** *Radiat Oncol* 2006, **1**:37.
38. Moseley DJ, White EA, Wiltshire KL, Rosewall T, Sharpe MB, Siewerdsen JH, Bissonnette JP, Gospodarowicz M, Warde P, Catton CN, Jaffray DA: **Comparison of localization performance with implanted fiducial markers and cone-beam computed tomography for on-line image-guided radiotherapy of the prostate.** *Int J Radiat Oncol Biol Phys* 2007, **67(3)**:942-53.
39. Nichol AM, Brock KK, Lockwood GA, Moseley DJ, Rosewall T, Warde PR, Catton CN, Jaffray DA: **A magnetic resonance imaging study of prostate deformation relative to implanted gold fiducial markers.** *Int J Radiat Oncol Biol Phys* 2007, **67(1)**:48-56.
40. Poggi MM, Gant DA, Sewchand W, Warlick WB: **Marker seed migration in prostate localization.** *Int J Radiat Oncol Biol Phys* 2003, **56(5)**:1248-51.
41. Kitamura K, Shirato H, Shimizu S, Shinohara N, Harabayashi T, Shimizu T, Kodama Y, Endo H, Onimaru R, Nishioka S, Aoyama H, Tsuchiya K, Miyasaka K: **Registration accuracy and possible migration of internal fiducial gold marker implanted in prostate and liver treated with real-time tumor-tracking radiation therapy (RTRT).** *Radiother Oncol* 2002, **62(3)**:275-81.
42. Beltran C, Herman MG, Davis BJ: **Planning target margin calculations for prostate radiotherapy based on intrafraction and interfraction motion using four localization methods.** *Int J Radiat Oncol Biol Phys* 2008, **70(1)**:289-95.